Structure, Vol. 12, 1303–1311, July, 2004, ©2004 Elsevier Ltd. All rights reserved. DOI 10.1016/j.str.2004.04.014

Crystal Structure of the Kinase Domain of WNK1, a Kinase that Causes a Hereditary Form of Hypertension

Xiaoshan Min,[1] Byung-Hoon Lee,[2] Melanie H. Cobb,[2] and Elizabeth J. Goldsmith[1,*]
[1]Department of Biochemistry
[2]Department of Pharmacology
University of Texas Southwestern Medical Center at Dallas
5323 Harry Hines Boulevard
Dallas, Texas 75390

Summary

WNK kinases comprise a small group of unique serine/threonine protein kinases that have been genetically linked to pseudohypoaldosteronism type II, an autosomal dominant form of hypertension. Here we present the structure of the kinase domain of WNK1 at 1.8 Å resolution, solved in a low activity conformation. A lysine residue (Lys-233) is found in the active site emanating from strand β2 rather than strand β3 as in other protein kinases. The activation loop adopts a unique well-folded inactive conformation. The conformations of the P+1 specificity pocket, the placement of the conserved active site threonine (Thr-386), and the exterior placement of helix C, contribute to the low activity state. By homology modeling, we identified two hydrophobic residues in the substrate-binding groove that contribute to substrate specificity. The structure of the WNK1 catalytic domain, with its unique active site, may help in the design of therapeutic reagents for the treatment of hypertension.

Introduction

Protein kinases are central signal transducers involved in control of all facets of cell function, including changes in the cellular program as well as cellular homeostasis. Recently, the human protein kinase superfamily was estimated to possess just over 500 members (Kostich et al., 2002; Manning et al., 2002), which were classified into seven major groups. In addition, a few less populated groups have been identified. WNK kinases (*w*ith *n*o lysine [*K*]) (Xu et al., 2000, 2002) comprise a very small group which have gained attention recently because two of its members have been shown to be mutated in a form of Mendelian hypertension (Wilson et al., 2001).

WNK kinases are unique among protein kinases in lacking a conserved lysine residue (Lys-72 in cAMP-dependent protein kinase [PKA]) (Knighton et al., 1991) from strand β3 (subdomain II, nomenclature defined in Hanks and Hunter [1998]), the residue most often mutated to generate inactive protein kinases (Robinson et al., 1996). In WNK kinases, this lysine is replaced by a cysteine. Nevertheless, at least two of the known WNK kinases have been shown to possess protein serine/threonine kinase activity, and model-building and mutagenesis analysis revealed that a different lysine residue in strand β2 (subdomain I) was necessary for kinase activity (Xu et al., 2000). The kinase domains of the WNK kinases possess no more than 29% (to Ste20) sequence identity with other protein kinases. They are found only in multicellular organisms (Verissimo and Jordan, 2001; Xu et al., 2000); there are four homologs in human, at least two in rat and mouse, one in *C. elegans*, and *Drosophila*, and nine in *Arabidopsis thaliana*.

The physiological roles of WNK kinases were completely unknown until the recent findings that pseudohypoaldosteronism type II (PHAII), an autosomal dominant disorder featuring hypertension, was shown to be caused by mutations in two of the four human WNK kinases, WNK1 and WNK4 (Wilson et al., 2001). Given the sensitivity of PHAII patients to thiazide diuretics, an antagonist of the Na-Cl cotransporter (NCCT), it was postulated that upregulation of the NCCT could be the cause (Wilson et al., 2003; Yang et al., 2003). In studies directed toward understanding the roles of WNK1 and WNK4 in pseudohypoaldosteronism II, it was found that wild-type WNK4 reduced the levels of the Na-Cl cotransporter, when coexpressed in *Xenopus* ooccytes. The reduction in NCCT levels occurred only when using wild-type WNK4, but not with kinase-dead WNK4 or one of the disease-causing mutants (Q565E) (Wilson et al., 2003; Yang et al., 2003). The disease-causing mutations in WNK1 are large intronic deletions that increase its expression in kidney. When coexpressed with WNK4, WNK1 abolishes the inhibitory effect of WNK4 on NCCT, having no affect on the NCCT activity on its own (Yang et al., 2003). Thus, it appears that WNK1 and WNK4 have distinct and opposite roles in the regulation of ion homeostasis. WNK4 is highly expressed in kidney, and WNK1 is expressed ubiquitously. Using a yeast two-hybrid screen, Lee et al. showed that WNK1 binds to synaptotagmin 2, and in vitro assays showed that WNK1 phosphorylates synaptotagmin 2 (B.H.L. et al., submitted). Synaptotagmins are involved in membrane trafficking, and this activity could conceivably be involved in the mechanism by which WNK1 affects NCCT membrane expression levels. Xu et al. examined the ability of WNK1 to activate MAP kinases, and found that overexpressed WNK1, when cotransfected with ERK5, activates this MAP kinase, suggestive of roles for WNK1 other than in ion homeostasis (Xu et al., 2003).

The kinase domains of the four human homologs share approximately 80% sequence identity or better (Xu et al., 2000). Of the 2126 amino acids present in the originally cloned splice form of rat WNK1, the serine/threonine protein kinase domain is near the N terminus (amino acids 218–483). The sequence reveals relatively little secondary structure outside the kinase domain except two coiled-coil domains (amino acids 563–597 and 1814–1841) in the C-terminal extension. However, sequence conservation across species in the C-terminal extensions suggests biological functions for these segments. Deletion analysis revealed an autoinhibitory segment between residue 490 and 550 (Xu et al., 2002). This

*Correspondence: betsy@chop.swmed.edu

segment is predicted to have an α-helical secondary structure using Jpred (Cuff et al., 1998), but it lacks sequence identity to known domains. Mutagenesis analysis revealed that two phenylanaline residues (Phe-524 and Phe-526) within the autoinhibitory domain were especially important to the autoinhibition. An autophosphorylation site (Ser-382) was identified in the activation loop of the kinase domain, and this autophosphorylation is required for the kinase activity (Xu et al., 2002).

To further understand the mechanism of specificity, regulation, and catalysis of WNK protein kinases, we have determined the structure of the kinase domain of WNK1. We succeeded in crystallizing the low activity conformation in which the activation loop phosphorylation site serine was mutated to alanine (WNK1 194-483 S382A). The structure revealed the novel location of the catalytic lysine in β2 (subdomain I). This unusual active site may be advantageous in the development of specific inhibitors targeted to WNK protein kinases. The low activity structure is maintained by WNK-specific interactions of the activation loop. The structure, together with positions of amino acid replacements between WNK1 and WNK4 which are known to have different substrates, suggested possible site of substrate interactions. Mutation of Val-318 and Ala-448 of WNK1 in the substrate binding groove predicted from PKA to those found in WNK4, abrogated binding to substrate synaptotagmin 2. The structure of WNK1 is also unique in that the N-terminal domain β sheet is formed into a near β barrel, through the addition of a β strand N-terminal to the canonical kinase core, and lengthening of three of the β strands.

Results and Discussion

Full-length rat WNK1 expresses poorly both in bacteria and in insect cells. A series of constructs that included the wild-type kinase domain or the mutant S382A that eliminated the phosphorylation site and flanking sequences of varying length were tested for expression in *E. coli* and crystallization. One construct, containing residue 194–483 with the mutation S382A, was crystallized (Figure 1A). The crystal belongs to space group P1 and there are two molecules in the asymmetric unit. Selenomethionine protein crystals diffract to a higher resolution than the native crystals. The structure was solved by the single-wavelength anomalous dispersion (SAD) method using a complete data set collected on a single selenomethionine crystal. The final structure was refined in REFMAC5 (Murshudov et al., 1997) to an R factor of 18.9% (R_{free} = 22.7%) with reasonable stereochemistry (Table 1). The model contains 542 amino acids from two WNK1 molecules and 351 water molecules. In one molecule, the first 17 residues at the N terminus and three residues at the C terminus are disordered. In the other molecule, the first 16 and last 2 residues are disordered. The average B factor of the model is 24 Å^2.

Topology of WNK1

The kinase domain of WNK1 shares 29% sequence identity with Ste20, and close to 25% identity with other kinase groups. The overall fold resembles other protein kinases with the typical dual domain architecture (Knighton et al., 1991) (Figure 1C). However, the N-terminal domain is unique in having a six-stranded β sheet that is rolled up to form a nearly complete β barrel. This contrasts with the five-stranded β sheet found normally. The additional strand (labeled β_0) (Figure 1B and 1C) makes antiparallel β sheet hydrogen bonding interactions with β1 and part of the activation loop from the second molecule in the asymmetric unit (between residues 380 and 383). Three of the canonical strands, β1, β4, and β5, are longer than normal, promoting the near β barrel. The phosphate anchor ribbon, strands β1 and β2, adopt fairly normal positions, however. The C-terminal has a standard architecture, and in the construct we crystallized, there is no extension from the kinase core.

The Active Site

The WNK1 S382A mutant crystallized is inactive; autophosphorylation and activation is prevented by mutation of S382A. That the conformation is not active is most apparent because a highly conserved residue, Thr-386, corresponding to Thr-201 in PKA, is not in the active site. The position of Thr-386 is influenced by the conformation of the activation loop to which it is connected, and will be discussed below. Otherwise, much of the active site appears normal. Conserved catalytic residues in the catalytic loop (Asp-349, Lys-351, and Asn-354) (corresponding to Asp-166, Lys-168, and Asn-171 in PKA) adopt standard positions and peptide conformations. However, each of these residues adopts different side chain conformations such that the hydrogen bonding interactions expected on the basis of other kinase structures are not formed (Figure 2A).

The defining feature of the WNK kinase group is that they lack a catalytic lysine residue (Lys-72 in PKA) in strand β3 (subdomain II). This lysine residue normally forms an ion pair with a glutamic acid in helix C (Glu-91 of PKA) in active protein kinases (Bossemeyer et al., 1993; Knighton et al., 1991). The lysine residue also contacts the α- and β-phosphates of ATP, suggesting that the lysine-glutamate pair may be involved in protonating product ADP, or performing some other acid base function. In WNK1, a cysteine residue (Cys-250) occupies this position in strand β3 (subdomain II). However, the side chain of the cysteine residue is far from the active site, not likely a candidate for catalysis. A lysine residue (Lys-233) in strand β2 (subdomain I) reaches into the active site. Previously, we showed by mutagenesis that mutation of Lys-233 abolished kinase activity (Xu et al., 2000). The structure confirms that the catalytic lysine in WNK1 is located in strand β2, not in β3 as in other protein kinases (Figure 2).

Interestingly, WNK1 does possess the glutamate residue in helix C (Glu-268) that usually forms an ion pair with the catalytic lysine, but here it does not form ion pair with Lys-233. Instead it is 13 Å away, and forms a different ion pair with Arg-348 of the catalytic loop, and a hydrogen bond with Thr-373 in the activation loop helix 3_{10}-L_{12} (Figure 3). The normal lysine-glutamate pair is also not present in low activity CDK2 (De Bondt et al., 1993). To assess the function of this conserved gluta-

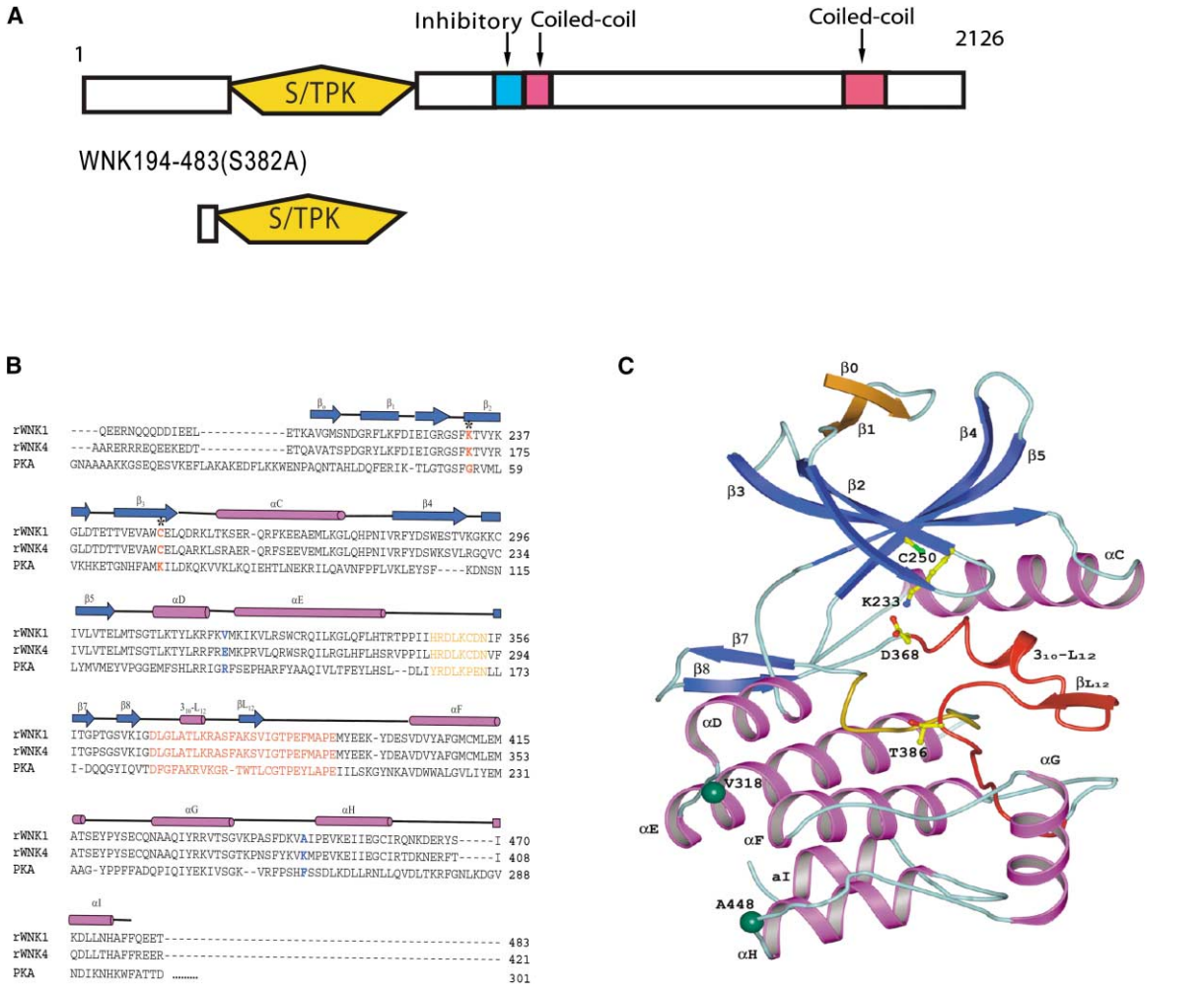

Figure 1. General Topology of WNK1 Kinase Domain

(A) Schematic diagram of the WNK1 domain organization and the construct used in the crystallization. S/TPK, serine/threonine protein kinase domain; CC, coiled-coil domain; Inh, autoinhibitory domain.

(B) Multiple sequence alignment of WNK1, WNK4, and cAMP-dependent protein kinase (PKA). Secondary structures are shown at the top of the alignment. The nomenclature for the secondary structure elements follows that for PKA structure. The helix A and B, strand 6 and 9 are not present. The sequences of the activation loop and catalytic loop are shown in red and yellow, respectively. The catalytic lysine Lys-233 and the typical lysine position residue Cys-250 in WNK1 are highlighted in red and marked with asterisks. Val-318 and Ala-448 are colored blue.

(C) Ribbon representation of WNK1. The five conserved β strands are blue and α helices are magenta. The extra N-terminal β strand is shown in gold. The activation loop is shown in red and the catalytic loop in yellow. Lys-233, Cys-250, Asp-368, and Thr-386 are shown in ball-and-stick representation. The green balls represent two substrate-specificity determinant residue Val-318 and Ala-418. The figure is prepared using Molscript (Kraulis, 1991) and GL-Render (L. Esser, personal communication). The multiple sequence alignment is prepared using T-Coffee (Notredame et al., 2000).

mate, we mutated Glu-268 to glutamine. The mutant could not be expressed, suggestive of an important role for this residue in stabilizing the structure. However, the results leave open the question of whether Glu-268 has a catalytic function.

The unique catalytic residue, Lys-233, contributes to the different shape of the ATP binding site. A large cavity is present in the back of the active site and near Cys-250. Further in the ATP binding site a glutamate residue (Glu-127 of PKA), which binds to ATP in many protein kinases, is replaced by a threonine residue (Thr-308) in WNK1, suggesting that ATP must be bound somewhat differently in WNK kinases. On the other hand, the backbone of the crossover connection, which in other kinases binds the adenine ring of ATP, looks similar to PKA.

Conformation of the Activation Loop

The unphosphorylated activation loop in the S382A mutant of WNK1 crystallized is well ordered throughout and maintains a low activity conformation through interactions at both ends of the loop. First, at the N terminus of the activation loop a two-turn 3_{10}-helix is formed (3_{10}-L_{12}) (Figure 3). This 3_{10}-helix is wedged between Phe-232 at the tip of the phosphate anchor ribbon and helix C, displacing helix C and Glu-268, from the catalytic cleft. The contact between the helix 3_{10}- L_{12} and helix C

Table 1. Details of Data Collection and Structure Determination for the Selenomethionine WNK1

Space group	P1
Unit cell	a = 38.30 Å, b = 57.77 Å, c = 65.66 Å, α = 91.3°, β = 89.99°, γ = 90.89°
Resolution (Å)	50–1.8 (1.86–1.8)[a]
Observed reflections	217,158 (21,551)
Unique reflections	50,614 (5,012)
Redundancy	4.3 (4.3)
Completeness	97.6% (96.9%)
R_{merge}[b]	0.077 (0.144)
$I/\sigma I$	27.9 (10.7)
R_{cryst}[c]	0.189
R_{free}[d]	0.228
Number of groups	
Protein atoms	4,706
Water	345
Rmsd in bond lengths (Å)	0.010
Rmsd in bond angles (°)	1.18
Average B factor (Å^2)	24.02
Ramachandran statistics (%)	
Most favored regions	90.7
Additional allowed regions	8.0
Generously allowed regions	0.6
Disallowed regions[e]	0.6

[a] Values between parentheses are for the highest resolution shell.
[b] $R_{merge} = \Sigma|(I_{hkl}) - <I>|/\Sigma(I_{hkl})$, where I_{hkl} is the integrated intensity of a given reflection.
[c] $R_{cryst} = \Sigma||F_{obs}| - k|F_{calc}||/\Sigma|F_{obs}|$, where F_{obs} and F_{calc} are the observed and calculated structure factors, respectively.
[d] R_{free} is calculated as R_{cryst} using 5% of the reflection data chosen randomly and omitted from the refinement calculations.
[e] Supported by excellent electron density.

is primarily hydrophobic and involves Phe-265 and Leu-272 in helix C, and Leu-369 and Leu-374 in helix 3_{10}-L_{12}. Leu-374 in helix 3_{10}-L_{12} also contacts Phe-232 in the phosphate anchor ribbon. The observed conformation is supported by interactions between Thr-373 of helix 3_{10}-L_{12}, Glu-268 in helix C, and Arg-348 in the catalytic loop (RD motif) (as noted above). Arg-348, which in active protein kinases forms contacts with the activating phosphorylation site, adopts an unusual left-hand conformation ($\varphi = 82°$; $\psi = -17°$) in making the interaction. The structure of the N terminus of the activation loop has features in common with low activity CDK2 in which a helix (αL_{12}) displaces helix C from the active site destroying the catalytic lysine-glutamate ion pair (De Bondt et al., 1993).

Second, the C terminus of the activation loop adopts a unique inactive conformation. The conserved residue Thr-386 (corresponding to Thr-201 in PKA) is displaced about 10 Å from its expected position (Figure 4A). The remodeling extends into the bottom of the P+1 site (expected by homology to be formed by residues Val-383 to Met-390). The last remodeled residue is Phe-389 in the sequence VIGTPEFMAPE, and Met-390 adopts a normal position. Remodeling of the P+1 pocket occurs in the low activity forms of p38 (Wang et al., 1997) and PAK1 (Lei et al., 2000); the remodeling here is unique however. The activation loop makes extensive van der Waals contacts with the linker (L_{14}) between helices F and G and the beginning of helix G involving the Val-383 and Pro-387 in the loop. This represents an outward displacement of the activation loop that creates another large unique cavity adjacent to the active site.

Wild-type WNK1 kinase domain becomes autophosphorylated when expressed in both *E. coli* and insect cells. From structural studies on other protein kinases determined in active conformation, it is known that the phosphorylated residue bound in a positively charged pocket that forms in the subunit interface, for example His-87, Arg-165, and Lys-189 in PKA, stabilizes the phosphorylated residue Thr-197 (Bossemeyer et al., 1993; Knighton et al., 1991) (Figure 4B). These residues are conserved in WNK kinases, suggestive that WNK kinases are activated by a similar mechanism. In the low activity structure determined here, none of the putative phosphate ligands is formed into a pocket: Lys-375 (corresponding to Lys-189 in PKA) interacts with catalytic aspartic acid Asp-348. Arg-264 (corresponding to His-87) is solvent exposed. Arg348 (corresponding to Arg-165) interacts with conserved glutamate Glu-268 in helix C.

The activation loop of WNK1 forms extensive interactions with the N-terminal domain of the neighboring molecule in the crystal (discussed below). This affects the position of four residues (Ala-380 to Val-383). However, the configuration of most part of the activation loop is not directly affected by this intermolecular interaction. Also, the intramolecular interactions at both ends of the activation loop are extensive, apparently having dominating roles in stabilizing the conformation, suggesting that they are not artifacts of the crystallization.

An Extensive Lattice Contact

Two molecules of WNK1 in the unit cell form an unusual crystal contact: the activation loop of a neighboring molecule is inserted between β4 and β0 in the N-terminal domain to complete the β barrel noted above (Figure 5). Four residues, Ala-380′, Lys-381′, Ala-382′ (S382A, mutated phosphorylation site), and Val-383′ (prime refers to the residue in the neighboring molecule) from the activation loop of a neighboring molecule, form β sheet hydrogen bonds with Val-212 and Met-214 in β0, and Glu-288 and Thr-290 in β4. The sheet is not continuous, however; one end of the strand is interacting only with β0 and the other only with β4. The interaction surface also includes αG, the loop connecting αC and β4, which interacts with the β4/β5 loop and β2/β3 loop from the second molecule respectively.

The two molecules in the asymmetric unit are similar but not identical. Superposition of the N-terminal domains and C-terminal domains of the two molecules gives a root-mean-square deviation (rmsd) of 1.0 and 0.6 Å respectively, whereas the overall superposition is worse, 1.3 Å, due to small differences in domain orientation. The larger rmsd between N-terminal domains is mainly due to differences in the lattice contacts.

The lattice contact interaction is present for each molecule in the crystal lattice. The patterns of interactions are also similar for each molecule in the lattice. Such interactions apparently do not occur in solution since WNK1 kinase domain is soluble and monomeric as assessed by gel filtration. The lattice provides a glimpse of how the activation loop of kinases becomes extended to bind in the active site of another kinase to become phosphorylated and is reminiscent of the CDK2-KAP complex (Song et al., 2001) (Figure 5). Considering the

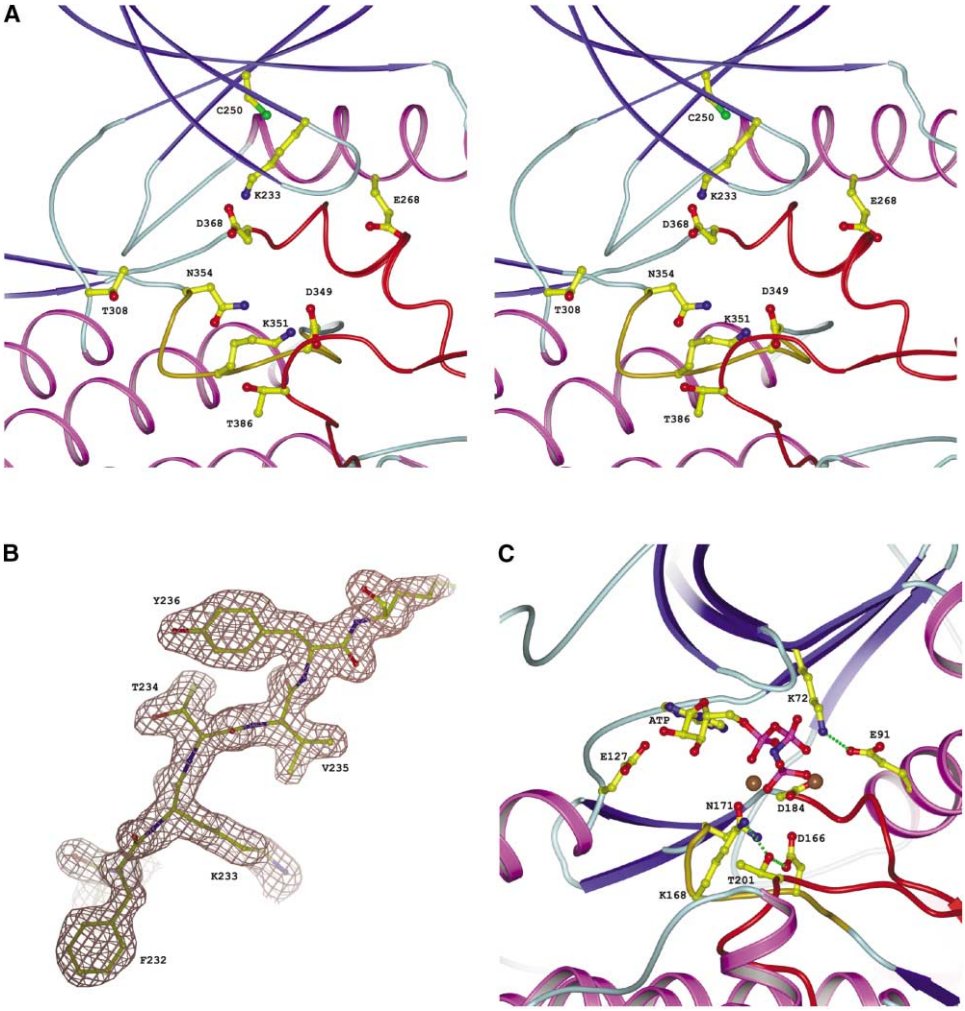

Figure 2. Comparison of the Active Site of WNK1 and PKA

(A) Stereo diagram of the active site of WNK1. Seven catalytic residues are shown in ball-and-stick representation.

(B) $2F_o - F_c$ electron density map of the phosphate anchor ribbon contoured at 1σ level.

(C) The active site of PKA. Residues corresponding to WNK1 are shown in ball-and-stick representation. The ion pair interactions between Lys-72 and Glu-91 and the hydrogen bonds between Thr-201 and Lys-168 and Asp-166 in PKA are displayed in green dotted lines. These interactions are not present in WNK1.

lattice contact from the point of view of the N-terminal domain β sheet, it is not known whether the contact is a mimic for substrate or autoinhibitory interactions.

Substrate Binding Site and Specificity

In a yeast two-hybrid study directed toward identifying possible physiological substrates of WNK1, Lee et al. showed that synaptotagmin 2, a calcium sensor protein involved in membrane trafficking, binds to WNK1 (B.H.L. et al., submitted). Using different fragments of synaptotagmin 2, it was shown that WNK1 interacts with the C2 domain of synaptotagmin 2. This interaction is specific for WNK1; the closely related WNK4 (83% identity in the kinase domain) does not bind synaptotagmin 2 in a two-hybrid test (B.H.L. et al., in submitted). We examined the kinase activity of WNK1 and WNK4 on substrate synaptotagmin 2. WNK4 phosphorylates synaptotagmin 2 only poorly (Figure 6A). To gain insight into the basis for this difference in substrate specificity, we generated a homology-based structural model of WNK4 using the WNK1 coordinates based on the multiple sequence alignment (Figure 1B), and found two residues in the substrate binding groove that might be involved in substrate recognition. The two residues, Val-318 (in the loop between helices D and E) and Ala-448 (in the loop between helix H and Helix I), are replaced by glutamate and lysine respectively in WNK4 (Figure 1B). The WNK1 mutant (V318E/A448K) did not bind to synaptotagmin 2 C2A or C2B domains as assessed by direct yeast two-hybrid experiment, but retained binding to another protein found in the dual hybrid screen (B.H.L. et al., submitted). This suggests that the two residues play major roles mediating the stable binding between WNK1 and synaptotagmin 2.

We next examined the effect of these mutations on the phosphorylation reactions. The mutant WNK1 showed slightly higher autophosphorylation than wild-type (data not shown), suggesting that the mutant retained cata-

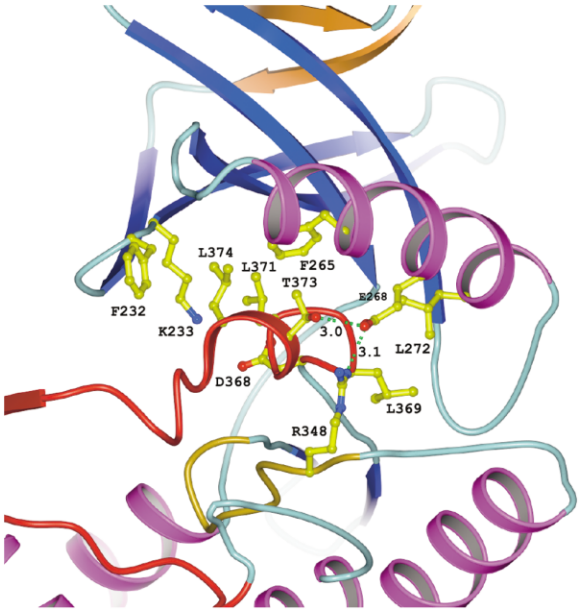

Figure 3. Extensive Interactions between the N-Terminal Helix of the Activation Loop with Helix C

Helices and strands are colored as in Figure 1.

lytic activity. The double mutation V318E/A448K in WNK1 decreased its activity toward specific substrate synaptotagmin 2 (40%–50%), although the activity is not as low as that of WNK4 (Figure 6B). Combining the stable binding assay and phosphorylation data, it is suggested that the two residues are important substrate specificity determinants that mediates the specific interactions between WNK1 and synaptotagmin 2.

The structure of WNK1 solved is in low activity conformation, and the P+1 specificity pocket is not formed (Figure 4). Sequence similarity with PKA suggests that WNK1 probably has a hydrophobic binding pocket for the P+1 residue. From mass spectrometry, two phosphorylation sites in synaptotagmin 2 have been identified; one is followed by a leucine residue and another by a glutamate residue (B.H.L., submitted). Apparently, the P+1 residue is not a strong specificity determinant for WNK1.

Conclusions

As anticipated from the sequences of WNK kinases and biochemical studies, WNK1 indeed does not have the catalytic lysine in β3 (subdomain II) common to all of the major groups of protein kinases, but instead possesses a catalytic lysine in β2 (subdomain I, Lys-233). The functional significance of the catalytic lysine placement in WNK1 is unknown. It is interesting that WNK1 kinase phosphorylates synaptotagmin 2 C2 domains. This well-folded substrate is different from many protein kinase substrates in which the sites of phosphorylation are in extended polypeptides or in very long loops that can be remodeled to bind in the active site of the protein kinase. The placement of the catalytic lysine may be necessary for alignment of its well-folded substrate into the kinase active site. Coincidently, a very distant homolog of protein kinases, aminoglycoside kinase APH(3′)-IIIa, has lysine residues in both β2 and β3 position (Hon et al., 1997). The position of catalytic lysine in β2 in WNK kinases may be related to some yet to identified regulatory mechanism. In any case, the different active site of WNK1 should be helpful in development of WNK1-specific inhibitors.

The extent of remodeling of the activation loop of WNK1 is also interesting. The low activity forms of most protein kinases are remodeled at either one end of the loop or the other. For example, low activity CDK2 has conformational changes in the N terminus of the loop, affecting helix C (De Bondt et al., 1993; Jeffrey et al., 1995), and MAP kinases have changes at the C terminus

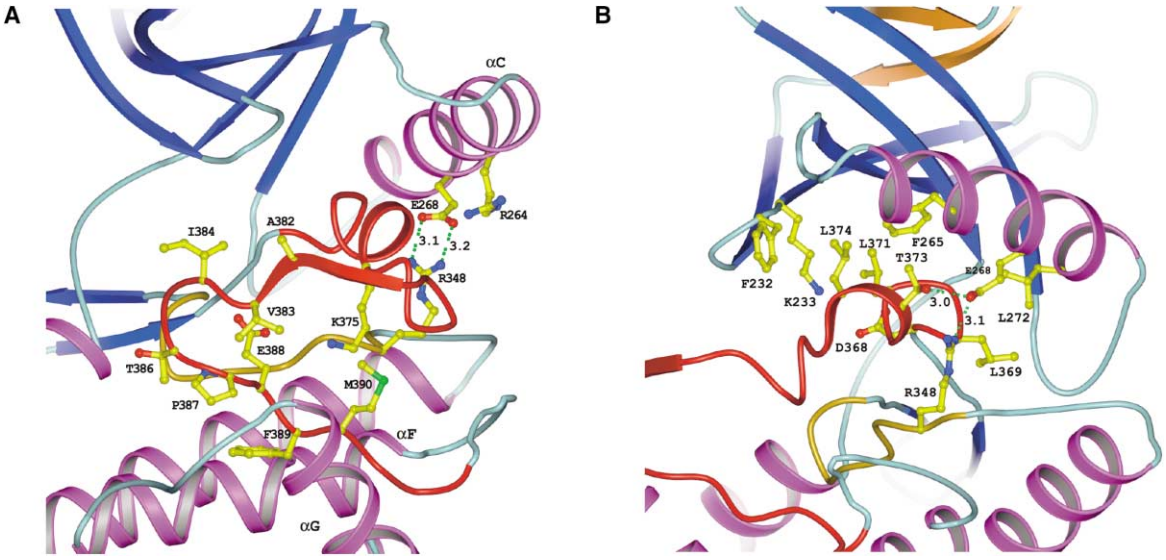

Figure 4. Conformation of the C Terminus of the Activation Loop

The P+1 site residues and positive charge residues that bind phosphate group of WNK1 (A) are compared with PKA (B).

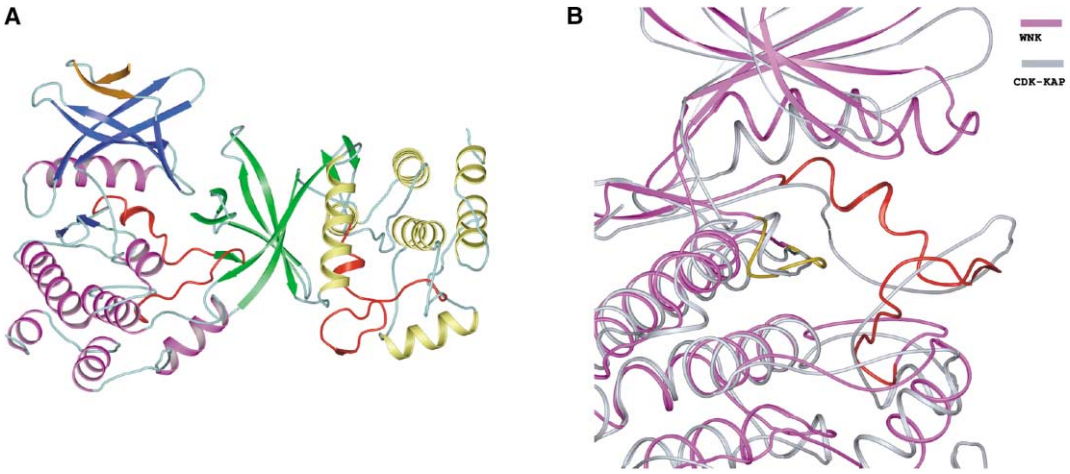

Figure 5. The Lattice Contact Interactions in WNK1

(A) One of the WNK1 lattice contact interactions. One molecule is colored as in Figure 1. The second molecule is displayed with green β strands and gold α helices. The interface consists of the activation loop of the first monomer and the N-terminal domain of the second.

(B) Structural superposition of WNK1 with CDK2 in complex with specific phosphatase KAP. WNK1 is shown in magenta. The activation loop and catalytic loop of WNK1 are highlighted in red and yellow respectively. CDK2 is colored in gray. The structure of KAP is removed for better view of the activation loop of CDK2.

(Canagarajah et al., 1997; Zhang et al., 1994), affecting the conserved threonine and the P+1 specificity pocket. Low activity WNK1 has both of these changes. In this respect, WNK1 resembles PAK1 which is also remodeled throughout the activation loop (Lei et al., 2000). The exterior position of the activation loop, apparently promoted by a lattice contact, offers a glimpse of how a kinase activation loop can fit into the active site of another enzyme for phosphorylation or dephosphorylation. The large cavity created in this conformation may offer further opportunities for drug development.

WNK kinases are regulated by autoinhibition from sequences outside the kinase domain. Also, WNK1 may be present in a large protein complex in the cell (our

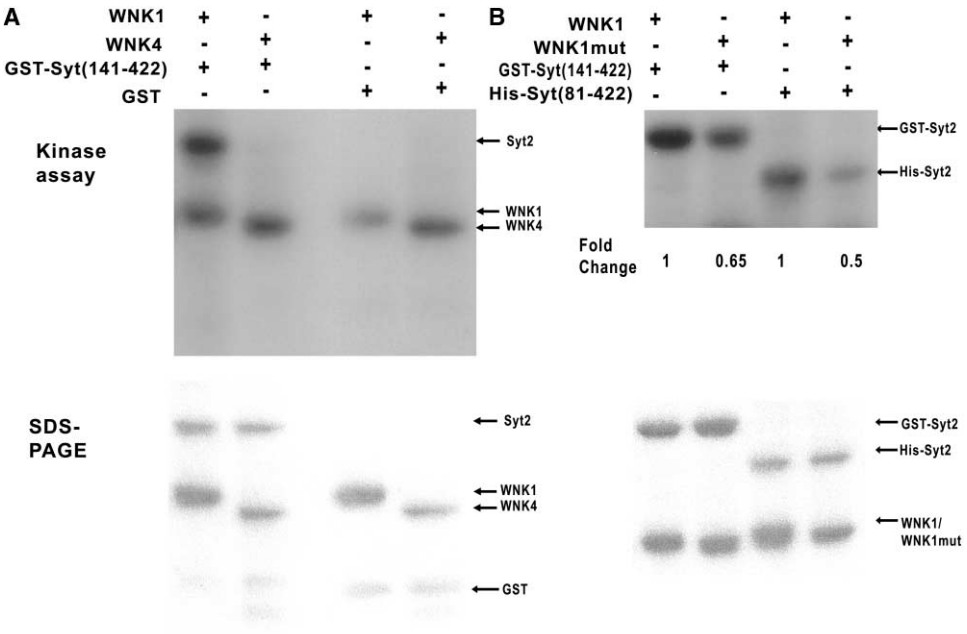

Figure 6. Substrate Specificity Determinant in WNK1

(A) Top panel, WNK1 (194-483) and WNK4 (141-436) were used in kinase assays with GST-syt2 (141-422) as substrate. The phosphorylation of GST-syt2 (141-422) and autophosphorylation of WNK1 and WNK4 are shown. Bottom panel, SDS-PAGE of the kinase assay.

(B) Top panel, wild-type WNK1 (194-483) and mutant WNK1 (194-483 V318E/A448K) were used in kinase assay with GST-syt2 (141-422) and His-syt2 (81-422) as substrates. The phosphorylations of both synaptotagmins are shown and the fold changes of the phosphorylation reactions are labeled below the autoradiogram. Bottom panel, SDS-PAGE of the kinase assay.

unpublished data). Thus, further studies are required to understand how this unusual serine/threonine protein kinase is regulated. Perhaps these other interactions will offer further clues concerning the function of the lysine in β strand 2.

Experimental Procedures

Expression and Purification of WNK Kinase Domain

The kinase domain of WNK1 (residues194–483) was cloned into a pHisParallel vector (Sheffield et al., 1999) with a TEV cleavage site between the fusion protein and His_6 tag. The autophosphorylation site S382 was mutated to an alanine using the Quik-change method (Stratagene). The protein was expressed in Rosetta (DE3) cells (Novagen). The cells were induced with 1 mM IPTG at $OD_{600} = 0.5$ and the protein was expressed for 20 hr, 20°C. Cells were lysed in two passes through an Avestin cell disruptor. The lysate was cleared by centrifugation at 35,000 × g for 1 hr. The supernatant was applied to a fast-chelating sepharose column (Amersham Pharmacia) precharged with 0.1 mM $NiSO_4$ and protein eluted with 250 mM imidazole. The fraction containing WNK1 was incubated with TEV protease overnight and purified in a second pass on the Ni-charged sepharose column. WNK1 (194-483 S382A) was further purified on a Mono-Q HR5/5 column (Amersham Pharmacia), using a linear gradient, and then by size-exclusion chromatography on Superdex-75 16/60 column equilibrated with 50 mM Tris, pH 8.0, 100 mM NaCl, 0.5 mM EDTA, and 1 mM TCEP (tris(2-carboxyethyl)phosphine; Sigma). The protein was concentrated to 10 mg/ml before crystallization. The selenomethionine incorporated protein was expressed in *met* auxotrophic strain B834 (Novagen) grown in minimum media supplemented with selenomethionine and other nutrients (Doublie, 1997) and purified using the same protocol as for native protein.

Crystallization and X-Ray Data Collection

Crystals were grown by hanging-drop vapor diffusion method at 16°C. The well solution contains 24% PEG monomethyl ester 2000, 300 mM NaCl, and 100 mM HEPES. Crystals appeared in a range of pH from 7.0 to 8.0. Crystals were grown initially by mixing 2 μl of the well solution with 2 μl of the protein to form the hanging drop. The crystal appeared overnight and grew to dimensions 100 × 100 × 200 μm in 3 days. The selenomethionine protein crystallized in the same condition. The crystals were transferred stepwise into a stabilizing solution containing 15% glycerol, 26% PEG monomethyl ester 2000, and 300 mM NaCl, pH 7.5. The crystals were flash frozen in liquid propane. Diffractions were collected at APS beamline 19-BM. Data were integrated and scaled using the HKL2000 program (Otwinowski and Minor, 1997).

Structure Determination and Refinement

Seventeen out of twenty selenomethionine sites were located using the automatic structure determination package SOLVE/RESOLVE (Terwilliger and Berendzen, 1999). The phases obtained from SOLVE were further improved by solvent flattening and histogram matching with a solvent content of 45%, using the program DM (Cowtan, 1994) in the CCP4 package (CCP4, 1994). The initial map after phase improvement was of excellent quality and readily interpretable. The program ARP/wARP was used to automatically build the main chains and side chains of the initial model (Perrakis et al., 1997, 1999). Out of 590 residues of the total protein, 530 residues were positioned automatically by the program. The remainder of the model was manually built using the program O (Jones et al., 1991). Crystallographic refinement was carried out with maximum likelihood target using the program REFMAC5 (Murshudov et al., 1997). The refinement statistics are summarized in Table 1.

Protein Purification and Kinase Assay

Rat WNK4 kinase domain (141-436) was cloned into baculovirus and expressed in insect cells using the GIBCO/Life Technologies procedures. His-tagged synaptotagmin 2 (81-422) and GST-tagged synaptotagmin 2 (141-422) were prepared as described (Shao et al., 1996). All of the mutants of WNK1 were generated using the Quikchange method (Stratagene). Standard kinase assays were performed in 30 μl of kinase buffer (20 mM HEPES, pH 7.6, 10 μM ATP, 10 μM 10 mM MgCl2, 10 mM β-glycerophosphate, 1 mM dithiothreitol, and 1 mM benzamidine) containing 10 μCi of [γ-^{32}P] ATP. Recombinant WNK1 and synaptotagmin 2 were added at final concentrations of 1 and 0.7 μM, respectively. Kinase reactions were terminated with 5μl SDS sample buffer followed by boiling 2 min.

Acknowledgments

We thank members of the Goldsmith lab for helpful discussions. We also thank Drs. Diana Tomchick and Mischa Machius and the staff at Argonne National Laboratory for help with Synchrotron data collection. We thank Dr. Dominika Borek for suggestions on data scaling. This research was supported by grants I1128 and I1143 from the Welch Foundation. Use of the Argonne National Laboratory Structural Biology Center beamlines at the Advanced Photon Source was supported by the U.S. Department of Energy, Office of Biological and Environmental Research, under Contract No.W-31-109-ENG-38.

Received: January 16, 2004
Revised: March 22, 2004
Accepted: April 9, 2004
Published: July 13, 2004

References

Bossemeyer, D., Engh, R.A., Kinzel, V., Ponstingl, H., and Huber, R. (1993). Phosphotransferase and substrate binding mechanism of the cAMP-dependent protein kinase catalytic subunit from porcine heart as deduced from the 2.0 Å structure of the complex with Mn2+ adenylyl imidodiphosphate and inhibitor peptide PKI(5-24). EMBO J. *12*, 849–859.

Canagarajah, B.J., Khokhlatchev, A., Cobb, M.H., and Goldsmith, E.J. (1997). Activation mechanism of the MAP kinase ERK2 by dual phosphorylation. Cell *90*, 859–869.

CCP4 (Collabrative Computational Project, Number 4) (1994). The CCP4 suite: programs for protein crystallography. Acta Crystallogr. D Biol. Crystallogr. *50*, 760–763.

Cowtan, K. (1994). Dm': an automated procedure for phase improvement by density modification. Joint CCP 4 and ESF-EACBM Newsletter on Protein Crystallography *31*, 34–38.

Cuff, J.A., Clamp, M.E., Siddiqui, A.S., Finlay, M., and Barton, G.J. (1998). JPred: a consensus secondary structure prediction server. Bioinformatics *14*, 892–893.

De Bondt, H.L., Rosenblatt, J., Jancarik, J., Jones, H.D., Morgan, D.O., and Kim, S.H. (1993). Crystal structure of cyclin-dependent kinase 2. Nature *363*, 595–602.

Doublie, S. (1997). Preparation of selenomethionyl proteins for phase determination. Methods Enzymol. *276*, 523–530.

Hanks, S.K., and Hunter T. (1995). Protein kinases 6. The eukaryotic protein kinase superfamily: kinase (catalytic) domain structure and classification. FASEB J. *9*, 576–596.

Hon, W.C., McKay, G.A., Thompson, P.R., Sweet, R.M., Yang, D.S., Wright, G.D., and Berghuis, A.M. (1997). Structure of an enzyme required for aminoglycoside antibiotic resistance reveals homology to eukaryotic protein kinases. Cell *89*, 887–895.

Jeffrey, P.D., Russo, A.A., Polyak, K., Gibbs, E., Hurwitz, J., Massague, J., and Pavletich, N.P. (1995). Mechanism of CDK activation revealed by the structure of a cyclinA-CDK2 complex. Nature *376*, 313–320.

Jones, T.A., Zou, J.-Y., Cowan, S.W., and Kjeldgaard, M. (1991). Improved methods for building protein models in electron density maps and the location of errors in these models. Acta Crystallogr. A *47*, 110–119.

Knighton, D.R., Zheng, J.H., Ten Eyck, L.F., Ashford, V.A., Xuong, N.H., Taylor, S.S., and Sowadski, J.M. (1991). Crystal structure of the catalytic subunit of cyclic adenosine monophosphate-dependent protein kinase. Science *253*, 407–414.

Kostich, M., English, J., Madison, V., Gheyas, F., Wang, L., Qiu, P.,

Greene, J., and Laz, T.M. (2002). Human members of the eukaryotic protein kinase family. Genome Biol. *3*, RESEARCH0043.

Kraulis, P.J. (1991). MOLSCRIPT: a program to produce both detailed and schematic plots of protein structures. J. Appl. Crystallogr. *24*, 946–950.

Lei, M., Lu, W., Meng, W., Parrini, M.C., Eck, M.J., Mayer, B.J., and Harrison, S.C. (2000). Structure of PAK1 in an autoinhibited conformation reveals a multistage activation switch. Cell *102*, 387–397.

Manning, G., Whyte, D.B., Martinez, R., Hunter, T., and Sudarsanam, S. (2002). The protein kinase complement of the human genome. Science *298*, 1912–1934.

Murshudov, G.N., Vagin, A.A., and Dodson, E.J. (1997). Refinement of macromolecular structures by the maximum-likelihood method. Acta Crystallogr. D *53*, 240–255.

Notredame, C., Higgins, D.G., and Heringa, J. (2000). T-Coffee: a novel method for fast and accurate multiple sequence alignment. J. Mol. Biol. *302*, 205–217.

Otwinowski, Z., and Minor, W. (1997). Processing of X-ray diffraction data collected in oscillation mode. Methods Enzymol. *276*, 307–326.

Perrakis, A., Sixma, T.K., Wilson, K.S., and Lamzin, V.S. (1997). wARP: improvement and extension of crystallographic phases by weighted averaging of multiple refined dummy atomic models. Acta Crystallogr. D Biol. Crystallogr. *53*, 448–455.

Perrakis, A., Morris, R., and Lamzin, V.S. (1999). Automated protein model building combined with iterative structure refinement. Nat. Struct. Biol. *6*, 458–463.

Robinson, M.J., Harkins, P.C., Zhang, J., Baer, R., Haycock, J.W., Cobb, M.H., and Goldsmith, E.J. (1996). Mutation of position 52 in ERK2 creates a nonproductive binding mode for adenosine 5′-triphosphate. Biochemistry *35*, 5641–5646.

Shao, X., Davletov, B.A., Sutton, R.B., Sudhof, T.C., and Rizo, J. (1996). Bipartite Ca2+-binding motif in C2 domains of synaptotagmin and protein kinase C. Science *273*, 248–251.

Sheffield, P., Garrard, S., and Derewenda, Z. (1999). Overcoming expression and purification problems of RhoGDI using a family of "parallel" expression vectors. Protein Expr. Purif. *15*, 34–39.

Song, H., Hanlon, N., Brown, N.R., Noble, M.E., Johnson, L.N., and Barford, D. (2001). Phosphoprotein-protein interactions revealed by the crystal structure of kinase-associated phosphatase in complex with phosphoCDK2. Mol. Cell *7*, 615–626.

Terwilliger, T.C., and Berendzen, J. (1999). Automated MAD and MIR structure solution. Acta Crystallogr. D *55*, 849–861.

Verissimo, F., and Jordan, P. (2001). WNK kinases, a novel protein kinase subfamily in multi-cellular organisms. Oncogene *20*, 5562–5569.

Wang, Z., Harkins, P.C., Ulevitch, R.J., Han, J., Cobb, M.H., and Goldsmith, E.J. (1997). The structure of mitogen-activated protein kinase p38 at 2.1-A resolution. Proc. Natl. Acad. Sci. USA *94*, 2327–2332.

Wilson, F.H., Disse-Nicodeme, S., Choate, K.A., Ishikawa, K., Nelson-Williams, C., Desitter, I., Gunel, M., Milford, D.V., Lipkin, G.W., Achard, J.-M., et al. (2001). Human hypertension caused by mutations in WNK kinases. Science *293*, 1107–1112.

Wilson, F.H., Kahle, K.T., Sabath, E., Lalioti, M.D., Rapson, A.K., Hoover, R.S., Hebert, S.C., Gamba, G., and Lifton, R.P. (2003). Molecular pathogenesis of inherited hypertension with hyperkalemia: the Na-Cl cotransporter is inhibited by wild-type but not mutant WNK4. Proc. Natl. Acad. Sci. USA *100*, 680–684.

Xu, B.-E., English, J.M., Wilsbacher, J.L., Stippec, S., Goldsmith, E.J., and Cobb, M.H. (2000). WNK1, a novel mammalian serine/threonine protein kinase lacking the catalytic lysine in subdomain II. J. Biol. Chem. *275*, 16795–16801.

Xu, B.-E., Min, X., Stippec, S., Lee, B.-H., Goldsmith, E.J., and Cobb, M.H. (2002). Regulation of WNK1 by an autoinhibitory domain and autophosphorylation. J. Biol. Chem. *277*, 48456–48462.

Xu, B.E., Stippec, S., Lenertz, L., Lee, B.H., Zhang, W., Lee, Y.K., and Cobb, M.H. (2003). WNK1 activates ERK5 by an MEKK2/3-dependent mechanism. J. Biol. Chem. *279*, 7826–7831.

Yang, C.-L., Angell, J., Mitchell, R., and Ellison, D.H. (2003). WNK kinases regulate thiazide-sensitive Na-Cl cotransport. J. Clin. Invest. *111*, 1039–1045.

Zhang, F., Strand, A., Robbins, D., Cobb, M.H., and Goldsmith, E.J. (1994). Atomic structure of the MAP kinase ERK2 at 2.3 Å resolution. Nature *367*, 704–711.

Accession Numbers

The coordinates have been deposited into the Protein Data Bank with accession code 1T4H.